

## Dielectric behaviour of strontium titanate glass ceramics with bismuth oxide addition as nucleating agent

O P Thakur<sup>\*</sup>, Devendra Kumar, Om Parkash<sup>#</sup> and Lakshman Pandey<sup>\*\*</sup>

Department of Ceramic Engineering, # School of Materials Science & Technology,  
Institute of Technology, Banaras Hindu University, Varanasi-221 005, India

<sup>\*\*</sup>Department of Physics, Rani Durgavati University, Jabalpur-482 001, India

Received 18 July 1996, accepted 8 November 1996

**Abstract** : Crystallization of perovskite strontium titanate phase in aluminosilicate and borosilicate glass ceramic systems is difficult. Crystallization occurred in complex manner with several silicate and borate phases which appear alongwith SrTiO<sub>3</sub>. Strontium titanate can be crystallized in a major amount in strontium titanate borosilicate glass ceramic system by suitable addition of alkali oxide K<sub>2</sub>O. Addition of Bi<sub>2</sub>O<sub>3</sub> as nucleating agent markedly affect the crystallization behaviour and resulting microstructure. In this paper, we are reporting the dielectric behaviour of strontium titanate borosilicate glass ceramic containing Bi<sub>2</sub>O<sub>3</sub> as nucleating agent. Different glass ceramic samples were crystallized in the temperature range 850°C to 950°C Dielectric characteristics were measured from room temperature to 250°C over a frequency range 100 Hz to 1 MHz. The magnitude of dielectric constant for glass ceramic sample no. C is higher ( $\approx 2500$ ). Impedance spectroscopic analysis of dielectric data has been carried out to investigate the contribution of crystal, glass and glass-crystal interface to the resulting dielectric behaviour of glass ceramics

**Keywords** : Dielectric, glass ceramics, immitance, microstructure

**PACS Nos.** : 81.05.Pj, 78.20.Ci, 81.40.Tv

### 1. Introduction

Over the last few decades, numerous attempts had been made to investigate and develop fine grained, pore-free glass ceramics containing BaTiO<sub>3</sub>, PbTiO<sub>3</sub>, NaNbO<sub>3</sub> ferroelectric phases [1–5] for different dielectric applications. The characteristics of these glass ceramics are tailored by suitable choice of parent glass composition and heat treatment schedule to control the constitution of crystalline phases and the microstructure.

<sup>\*</sup> Present Address : Ferrite Division, Solid State Physics Laboratory,  
Lucknow Road, Delhi-110 054, India

Reports are also available for strontium titanate aluminosilicate glass ceramics in various cryogenic capacitive applications [6]. Strontium titanate is a nonferroelectric perovskite ceramic. Suitable processing of these ceramics leads to the formation of barrier layers at grain boundaries and material-electrode interface. These barriers give rise to very high value of effective dielectric constant [7] and are used as a barrier layer capacitor. Crystallization of pure strontium titanate phase in aluminosilicate [8] and borosilicate [9] glass ceramics is quite complex and difficult. The crystallization depends on purity of raw materials *i.e.* impurity content and nucleation treatment [10]. Crystallization of strontium titanate *via* glass ceramic process is always associated with precipitation of some other phases. In strontium titanate aluminosilicate glass ceramics, hexacelsian ( $\text{SrAl}_2\text{Si}_2\text{O}_8$ ), fresnoite ( $\text{Sr}_2\text{TiSi}_2\text{O}_8$ ) and some other crystalline phase precipitate out along with  $\text{SrTiO}_3$  [9–12] whereas in strontium titanate borosilicate glass ceramic system  $\text{Sr}_2\text{B}_2\text{O}_5$ ,  $\text{Sr}_3\text{Ti}_2\text{O}_7$ ,  $\text{TiO}_2$  and some other phases crystallize out.

Recently, Thakur *et al* [13] reported that by suitable addition of  $\text{K}_2\text{O}$  in strontium titanate borosilicate glass ceramics, leads to the formation of  $\text{SrTiO}_3$  phase in a major amount when these glasses were ceramized at higher temperatures (950–1000°C). The crystallization takes place by initial phase separation of glasses into SrO,  $\text{Bi}_2\text{O}_3$  rich and  $\text{TiO}_2$  rich regions. At low temperature, first  $\text{Sr}_2\text{B}_2\text{O}_5$ ,  $\text{TiO}_2$  and  $\text{Sr}_3\text{Ti}_2\text{O}_7$  phases form. When crystallization temperature is increased,  $\text{Sr}_2\text{B}_2\text{O}_5$  and  $\text{Sr}_3\text{Ti}_2\text{O}_7$  phases react with  $\text{TiO}_2$  and form desired  $\text{SrTiO}_3$  perovskite phase. It has been found that the small amount addition of  $\text{Bi}_2\text{O}_3$  affects crystallization behaviour and resulting microstructure of glass ceramics. A little amount of  $\text{Bi}_2\text{O}_3$  in alkali containing strontium titanate borosilicate glass ceramics leads to the formation of relatively large crystals with special types of regular faceting of crystal surfaces [14]. Many times, unusual pentagonal faceting is observed in their microstructures for  $\text{SrTiO}_3$  crystals.

In this paper, we report the results of our investigation of dielectric and immittance behaviour of alkali ( $\text{K}_2\text{O}$ ) containing strontium titanate borosilicate glass ceramics with small amount of  $\text{Bi}_2\text{O}_3$  addition as nucleating agent showing major amount of  $\text{SrTiO}_3$  phase.

## 2. Experimental procedure

An alkali modified strontium titanate borosilicate glass ( $\text{K}_2\text{O}$ - $\text{SrO}$ - $\text{TiO}_2$ - $\text{B}_2\text{O}_3$ - $\text{SiO}_2$ ) has been prepared. A small amount of ( $\text{SrO}$ - $\text{TiO}_2$ ) has been replaced by  $\text{Bi}_2\text{O}_3$ . The crystallization behaviour of this glass has been reported earlier [14]. The heat treatment schedule for different glass ceramic samples are shown in Table 1.

Batches weighing 25 gms containing proportionate amount of chemicals  $\text{SrCO}_3$ ,  $\text{TiO}_2$ ,  $\text{SiO}_2$ ,  $\text{H}_3\text{BO}_3$ ,  $\text{K}_2\text{CO}_3$  and  $\text{Bi}_2\text{O}_3$  (purity 99%) were-mixed thoroughly in an agate mortar using acetone as grinding medium. Well homogenised powders were then transferred in high grade alumina crucible and heated to a temperature range 1000–1100°C. The molten mass was stirred thoroughly to ensure better homogenization of the melt. The melt was quenched by pouring into aluminium mould and quickly pressed with another

cooled aluminium plate to get specimen to uniform thickness. Thus obtained glass samples were annealed in preheated furnace for two hours in the temperature range 450–600°C.

**Table 1.** Heat treatment schedule, crystalline phases and density of glass ceramic samples.

Sample name	Heat treatment schedules				
	Heating rate (°C/min.)	Holding time (hrs)	Cryst. Temp. (°C)	Phases observed	Density (gm/cm <sup>3</sup> )
A	5	3	950	P + SB* + ST*	3.0123
B	5	3	900	P + SB + ST*	3.487
C	5	3	950	P + R*	3.7310
D	Direct	6	950	P + R	3.1770

\*--Minor phase

Phases abbreviated as : SB = Sr<sub>2</sub>B<sub>2</sub>O<sub>5</sub>, ST = Sr<sub>3</sub>Ti<sub>2</sub>O<sub>7</sub>, R = TiO<sub>2</sub> (rutile), P = SrTiO<sub>3</sub>

Amorphosity of the glass was checked by X-ray diffraction. The glasses were crystallized by heating the respective glass specimens at uniform rate to the heat treatment temperature soaking for specific period of time and thereafter cooling to room temperature in a programmable furnace. The glass ceramic samples B and C were crystallized at 900 and 950°C respectively. One of the glass ceramic sample D was crystallized by inserting glass specimen directly in a preheated furnace at its heat treatment temperature. There are two possible routes of the formation of SrTiO<sub>3</sub> derived from (i) Sr<sub>2</sub>B<sub>2</sub>O<sub>5</sub> and (ii) Sr<sub>3</sub>Ti<sub>2</sub>O<sub>7</sub>. If the kinetics of formations are different, then there is a possibility of change in the microstructure and dielectric behaviour of resulting glass ceramics.

X-ray diffraction patterns for glass and glass ceramic samples were recorded using Rich-Seifert ID 3000 diffractometer using Cu-K<sub>α</sub> radiation. The microstructures of resulting glass ceramics were observed using scanning electron microscope (Model PSEM 500) and optical microscope (Zeiss, Model 415). Samples were coated with silver paint on both surfaces and cured for 5 minutes at 600°C. Dielectric characterization was done on Impedance Analyzer (HP 4192A LF) as a function of frequency from room temperature to 250°C.

### 3. Results and discussion

The density of various glass ceramic samples are listed in Table 1. Table 1 also includes the density of base glass ceramic sample without Bi<sub>2</sub>O<sub>3</sub> for comparison. XRD patterns of glass ceramic samples of base glass composition (sample A) treated at 950°C, and glass with Bi<sub>2</sub>O<sub>3</sub> treated at 900°C (sample B) and 950°C (sample C) are shown in Figure 1. In all the samples, SrTiO<sub>3</sub> phase crystallizes as a major phase. In glass ceramic samples A and B, Sr<sub>2</sub>B<sub>2</sub>O<sub>5</sub> and Sr<sub>3</sub>Ti<sub>2</sub>O<sub>7</sub> phases are also present in smaller amount, while in glass ceramic sample C, TiO<sub>2</sub> (rutile) phase is present in trace amount and there is no indication of the presence of Sr<sub>2</sub>B<sub>2</sub>O<sub>5</sub> and Sr<sub>3</sub>Ti<sub>2</sub>O<sub>7</sub> phases. The crystallization behaviour and resulting microstructure of these glass ceramics are described in details elsewhere [14].

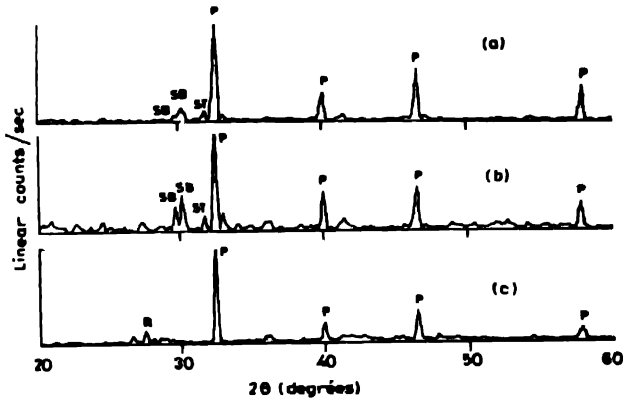


Figure 1. XRD patterns of glass ceramic sample nos. (a) A (base glass ceramic crystallized at 950°C) and glass ceramic with  $\text{Bi}_2\text{O}_3$ , (b) B (crystallized at 900°C), (c) C (crystallized at 950°C).

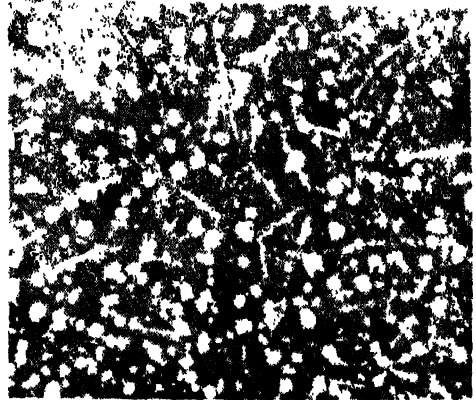
Representative optical and scanning electron micrographs are shown in Figure 2. The optical micrographs of glass ceramic sample B and C (Figures 2a and 2b) show different type of crystallization in different regions indicating phase separation occurring in these glasses. In  $\text{TiO}_2$ -rich phase,  $\text{Bi}_2\text{O}_3$  acts as a nucleating agent and  $\text{SrTiO}_3$  microcrystals grow directly. These micro-crystals have well-defined morphology and are faceted (Figure 2c) in contrast to the fine grained structure of the base glass ceramic A [13]. Crystallites size was found to be in the range 5–20  $\mu\text{m}$ .

The dielectric behaviour of base glass ceramic sample A is reported elsewhere [15] which is temperature independent with low value of dielectric constant. The magnitude of dielectric constant and dissipation factor falls in the range of 15–35 and 0.05–0.20 respectively.

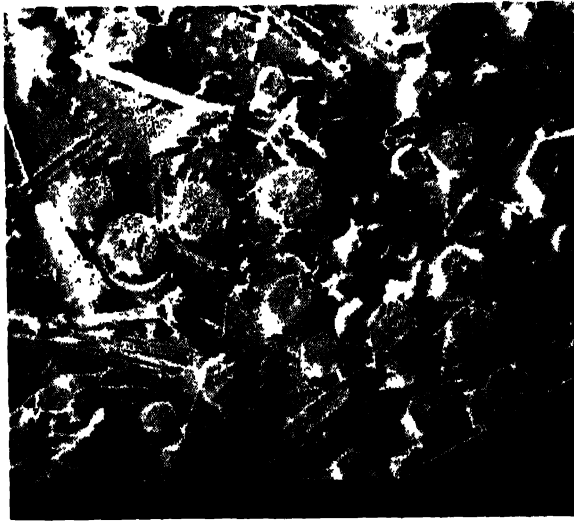
Dielectric behaviour at 1 KHz for glass ceramic samples B, C and D is shown in Figure 3. Dielectric constant of glass ceramic sample no. B lies in the range 100–250 with very little thermal variation. It shows lower value of dielectric loss. For the glass ceramic sample no. C, dielectric constant is observed to be very high in the range 600–2500. Dielectric constant increases with temperature. Same trend is observed for glass ceramic sample no. D with lower value of dielectric constant yielding 200–600. Figure 4 depicts the variation of dielectric constant and dissipation factor with respect to frequency. Dielectric constant dispersion is appreciable at lower frequency. The magnitude of dielectric constant is higher at lower frequency and at higher temperature which decreases with frequency. This may be ascribed to space charge polarization. The loss spectrum shows relax or behaviour containing two relaxation processes. Relaxation peaks shift towards higher frequency with respect to temperature. Loss spectrum at 511 K does not decrease in lower frequency region because of conduction losses.



(a)



(b)



(c)

Figure 2. Optical micrographs of glass  
SEM of (c) glass ceramic sample no. C.

le nos. (a) B, (b) C and



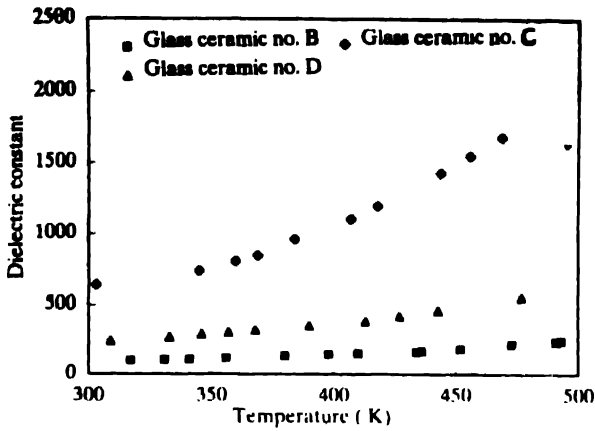


Figure 3. Variation of dielectric constant ( $\epsilon$ ) with temperature at 1 kHz for glass ceramic sample nos B, C and D.

An impedance spectroscopy technique has been widely exploited now-a-days in the field of electronic ceramics to separate out different contributions arising from grain, grain boundary and blocking electrode. To separate out the contribution of polarization processes

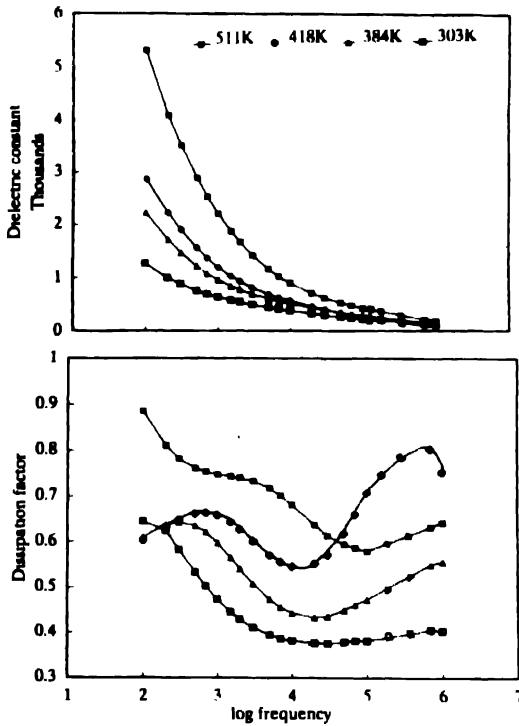


Figure 4. Variation of dielectric constant ( $\epsilon$ ) and dissipation factor ( $\tan \delta$ ) with frequency for glass ceramic sample no. C

of crystalline and glassy phase, impedance and modulus spectroscopic techniques have been applied [16,17]. An equivalent circuit consisting of R, C elements, can be selected on the basis of immittance plot at different temperatures. The nature of impedance plot

depends on the respective values of different R, C elements. In some cases, impedance plot describes detailed information about electrical components of ceramic samples; on the other hand, sometimes complex modulus plane formalism provides useful information about the same. It all depends on corresponding magnitude of R, C element. If the difference in the magnitude of resistance is greater for grain and grain boundary; complex impedance plot would highlight higher resistance contribution and shows single semicircular arc. In other words, lower resistance contribution will be suppressed by higher resistance value. Complex modulus plane plot highlights capacitive contribution and sensitive to lower magnitude of capacitance. It is wise to plot experimental data in various formalisms to avoid ambiguity in selection of proper equivalent circuit and hence magnitude of different R, C elements.

In present study, modulus plot is more relevant to extract the information about different components playing part in the electrical characteristics of glass ceramic samples. Table 2 contains resistance (R), capacitance (C) and time constant ( $\Gamma$ ) obtained from the intercept of modulus plots for different constituting components of glass ceramics.

For the glass ceramic sample no. B, complex impedance plane plot (Figure 5) shows a poorly resolved semicircle in higher frequency region which may be attributed to semiconducting crystallites whereas lower frequency region demonstrate nearly linear spike

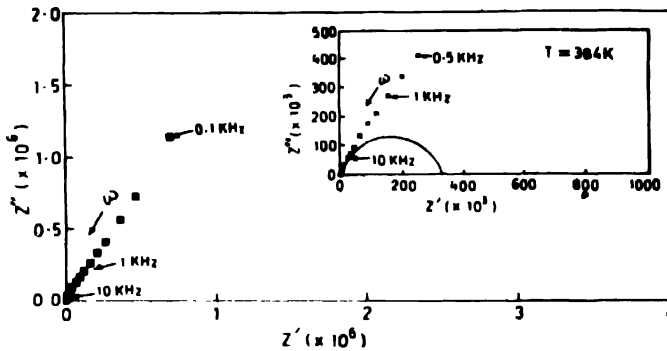


Figure 5. Complex impedance plane plot for glass ceramic sample no. C at 384 K.

corresponding to glassy region and glass-crystal interface. Spike at lower frequency region may be attributed to either very high resistance of its RC element or combination of RC element results in such a way that it falls out of the measurement scale. At higher temperatures, semicircle in high frequency region tends to diminish and eventually we have a complete spike inclined around  $45^\circ$ . In this case, modulus plots would be useful because  $C_2 = C_1$  and  $R_2/R_1 \approx 100$  [18].

Complex plane modulus plots of glass ceramic sample no. B at different temperatures as depicted in Figure 6, showing two depressed semicircles reveal distribution of relaxation times or more polarization processes are involved in polarization phenomenon. A comparison with figure corresponding to model circuits [17] reveals that the model circuit



Table 2. Values of R1, C1, R2, C2 and C3 obtained from complex modulus plane plots

Parameters calculated	Glass ceramic sample name											
	B			C			D					
	Temp. (K)	Temp. (K)	Temp. (K)	Temp. (K)	Temp. (K)	Temp. (K)	Temp. (K)	Temp. (K)	Temp. (K)	Temp. (K)	Temp. (K)	
	317	380	473	497	303	384	418	469	287	346	413	477
R1 (KΩ)	7.620	3.540	0.580	0.354	—	—	—	—	0.559	0.227	0.066	0.047
C1 (nF)	0.418	0.449	0.392	0.450	—	—	—	—	4.070	3.500	3.420	3.380
R2 (MΩ)	0.469	0.387	0.134	0.067	0.035	0.009	0.006	0.003	0.176	0.137	0.066	0.030
C2 (nF)	2.260	1.090	1.190	1.190	3.050	3.410	3.690	4.660	6.020	5.790	4.850	5.280
C3 (nF)	1.880	7.530	—	—	—	—	—	—	10.75	15.05	50.16	—
$\tau_1$ (μS)	3.183	1.591	0.227	0.159	—	—	—	—	2.270	0.790	0.226	0.159
$\tau_2$ (mS)	1.060	0.422	0.159	0.080	0.106	0.032	0.023	0.016	1.060	0.790	0.318	0.159

Note : R1, C1; R2, C2 and C3 are the resistance and capacitance from highest (crystalline phase), mid (glass and glass/crystal interface) and lowest frequency (electrode contribution) side respectively.  $\tau_1$  and  $\tau_2$  are the time constants, corresponding to higher and mid frequency region.

needed to represent this system would be similar to two parallel RC combinations ( $R_1, C_1; R_2, C_2$ ) connected in series with single capacitance  $C_3$ . The values of  $R_1, C_1; R_2, C_2$  and  $C_3$  are listed in Table 2. In our system, we have three contributions arising from blocking electrode, glass-crystal interface, glassy phase and crystalline phases which correspond to lower, mid and higher frequency region respectively. The data points shift towards lower frequency region with respect to temperature. Blocking electrode contribution observed to diminish at higher temperature which may be due to the decrement of total resistance of glass ceramic sample. From this study, it may be concluded that blocking electrode contribution probably arises because of non-ohmic contact with electrode material. The study of modulus spectra shows broad peak at lower temperature which narrowed down and tends to split into two peaks at higher temperature. Broad peak may be assigned to different time constants which have closer values or heterogeneous atmosphere contributing to this characteristics.

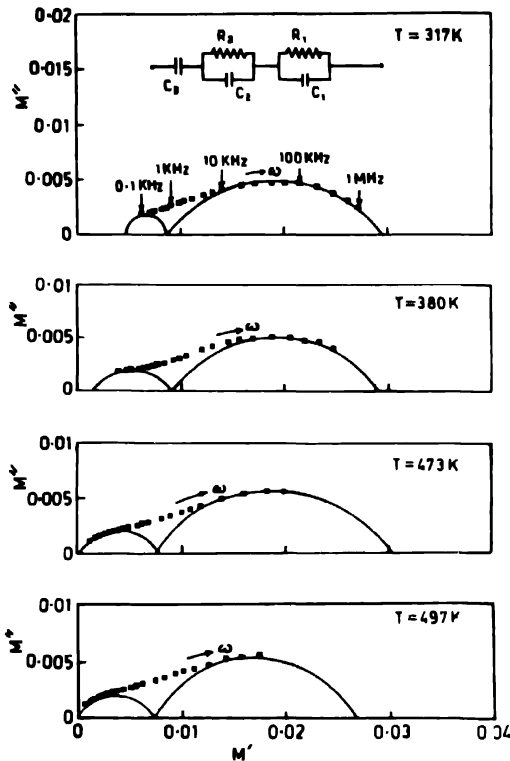


Figure 6. Complex modulus plane plots at different temperatures for glass ceramic sample no B

Complex plane impedance plot for glass ceramic sample crystallized at  $950^{\circ}\text{C}$  (sample C) shows the same nature as glass ceramic sample B. Modulus plane plots at different temperatures (Figure 7) represent single semicircle at lower frequency side and a spike at highest frequency region. Spike may be either due to very low value of resistance for this contribution or higher capacitance of crystalline phases. Depression in semicircular arc increases with temperature and data points shift towards lower frequency side. Blocking

electrode contribution becomes less appreciable at higher temperature. An equivalent circuit for this case may consist of two parallel RC elements connected in series with blocking electrode capacitance, in which capacitance, for crystalline phase (highest frequency side) is far higher than capacitance of glass and glass/crystal interface (lower frequency side).

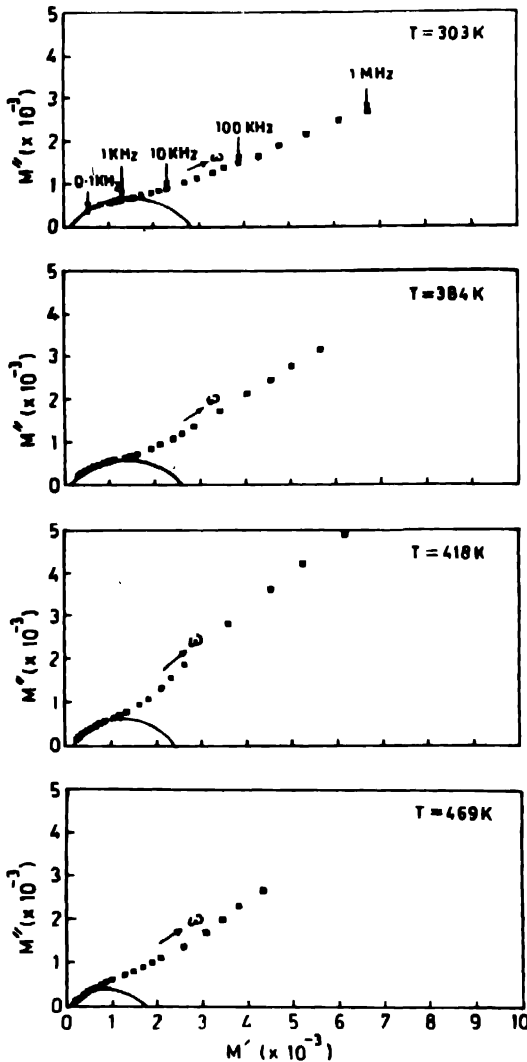


Figure 7. Complex modulus plane plots at different temperatures for glass ceramic sample no. C

Complex modulus plane plots at different temperatures for sample no. D are illustrated in Figure 8. It depicts two depressed semicircles showing distribution of relaxation times and electrode contribution. The difference in capacitance for these semicircles are less as compared to the modulus plane plots of glass ceramic no. B. The magnitude of capacitance and resistance of glass, glass/crystal interface and crystalline phases decreases with temperature. An electrode contribution gradually disappears at higher

temperature. An equivalent circuit for these contributions can be drawn as shown in the insert of Figure 8. Single capacitance C3 represents glass ceramic electrode contribution while two parallel RC elements, R1C1 and R2C2 reveal the contributions of glass, glass/crystal interface and crystalline phases respectively. In all glass ceramic samples, lower frequency arc in modulus plot shows combined effect of glassy phase and glass/crystal interfaces whereas highest frequency side arc shows the contribution from different crystalline phases embedded in glassy matrix.

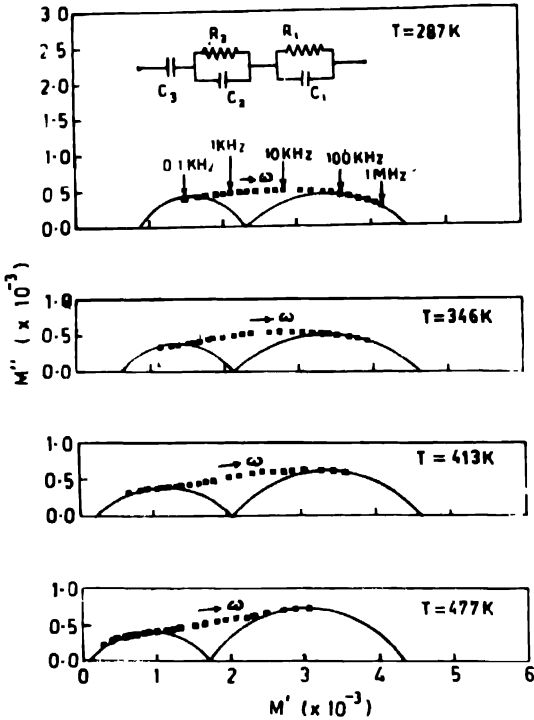


Figure 8. Complex modulus plane plots at different temperatures for glass ceramic sample no. D

The activation energy calculated from the temperature variation of resistivity of original base glass is found to be not equal to that of respective glassy phase obtained by complex impedance plots in different glass ceramic sample nos. B, C and D. The reason being that one does not know that how much fraction of SrO and TiO<sub>2</sub> had crystallized as SrTiO<sub>3</sub>, so it is difficult to find the exact composition of glassy matrix to be compared for.

In general, glass ceramics are composites consisting of one or more crystalline phases embedded in glassy matrix. An effective dielectric constant depends on the conductivity and capacitance of glassy matrix and different crystalline phases. It is observed that the dielectric constant for glass ceramic sample no. B is relatively lower than that of C and D which may be explained as follows : as can be seen from Table 2 that the magnitude of glass and glass/crystal interface resistance (R2) is higher than that of precipitated crystalline phases (R1). When a.c. signal is being applied to the glass ceramic specimen,

a meagre amount of charge starts migrating through glassy phase because of its higher resistance and there is little accumulation of charges at crystal/glass interface which results in low value of dielectric constant. As the temperature of measurements increases, conductivity of glassy phase as well as crystalline phase tends to increase with temperature which provides a little higher accumulation of charges which in turn, results in little higher value of dielectric constant at higher temperature. Capacitance for crystalline phases (C1) is lower than that of C2 (glass matrix and crystal-glass interface). Conductivity of both glassy and crystalline phase is slightly higher for glass ceramic sample no. D as evidenced from Table 2. The dielectric constant observed for glass ceramic sample no. D is higher than that of no. B because of the relatively higher values of C1 and C2. For glass ceramic sample no. C, higher value of effective dielectric constant results which may be due to the considerable reduction of resistance for glassy and crystalline phase which provide higher charge migration through specimen and larger amount of charge accumulation at glass/crystal interface. However, it is to be noted that the magnitude of resistance of glassy phase is three order higher than that of crystalline phase.

#### 4. Conclusions

In this glass ceramic system, strontium titanate was observed as a major phase at 950°C crystallization temperature which shows higher value of dielectric constant owing to space charge polarization. An immittance spectroscopic technique was applied to separate out the contributions of glassy matrix, glass-crystal interface and crystalline phases.

#### Acknowledgment

One of the authors (OPT) is highly thankful to the Department of Atomic Energy, Bombay, for awarding Dr. K S Krishnan research fellowship.

#### References

- [1] O Parkash, D Kumar and L Pandey *Bull. Mater. Sci.* **8** 557 (1986)
- [2] A Herczog *J. Am. Ceram. Soc.* **47** (3) 107 (1964)
- [3] A Herczog *J. Am. Ceram. Soc.* **67** 484 (1984)
- [4] D G Grossman and J O Isard *J. Am. Ceram. Soc.* **52** 230 (1969); *J. Phys.* **D3** 1058 (1970)
- [5] N F Borelli and M M Layton *J. Non-Cryst. Solids* **6** 197 (1971)
- [6] W N Lawless U.S. Patent No. 3 649891 (1972)
- [7] A Herczog *J. Am. Ceram. Soc.* **67** 484 (1984)
- [8] S L Swartz, E Breval, C A Randall and B H Fox *J. Mat. Sci.* **23** 3997 (1988)
- [9] O P Thakur, D Kumar, O Parkash and L Pandey *Bull. Mater. Sci.* **18** (5) 577 (1995)
- [10] S L Swartz and A S Bhalla *Mater. Res. Bull.* **21** 1417 (1986)
- [11] S L Swartz, E Breval and A S Bhalla *Am. Ceram. Soc. Bull.* **67** (4) 763 (1988)
- [12] O P Thakur, D Kumar, O Parkash and L Pandey *Bull. Mater. Sci.* **19** (2) 393 (1996)

- [13] O P Thakur, D Kumar, O Parkash and L Pandey *Mater. Lett.* **23** 253 (1995)
- [14] O P Thakur, D Kumar, O Parkash and L Pandey *Bull. Mater. Sci.* (Communicated)
- [15] O P Thakur, D Kumar, O Parkash and L Pandey *Indian. J. Pure Appl. Phys.* (Communicated)
- [16] J Ross McDonald *Impedance Spectroscopy* (New York : John Willey & Sons) (1987)
- [17] L Pandey, O Parkash, R Katore and D Kumar *Bull. Mater. Sci.* **18** (5) 563 (1995)
- [18] D C Sinclair and A R West *J. Appl. Phys.* **66** 3850 (1987)